'RESEARCH JOURNEY' International E- Research Journal
Vol. 10, Issue No. - 4 : Multidisciplinary Issue
Impact Factor 6.625 Peer Reviewed Journal
E-ISSN : 2348-7143
Oct.-Dec. - 2023

Spectral Properties of Rare-Earth-Doped and Co-Doped KMgF3 Phosphor Synthesis Via RAP

S. R. Jaiswal*[1], P. A. Nagpure[2]
[1] Department of Physics, Shri R. L. T. College of Science, Akola. 444001 (INDIA)
[2]Department of Physics, Shri Shivaji Science College, Amravati. 444602 (INDIA)

Highlights:

Rare-Earth-Doped and Co-doped KMgF3 Phosphor synthesis via reactive atmosphere process. The Quantum Efficiency (QE) was found to be 114% under the excitation at 246 nm in the Reactive Atmosphere Process (RAP).

Abstract:

In this work, we study the spectral properties of $KMgF_3$ doped and Co-doped Gd^{3+}, Eu^{3+} phosphor synthesis via Reactive Atmosphere Process (RAP). The powder X-ray diffraction (XRD) analysis illustrated purity in structure of synthesis phosphor. The photoluminescence (PL) emission and excitation spectra of $KMgF_3$:Gd^{3+} and Eu^{3+} were examined under VUV beamline of the Beijing Synchrotron Radiation Facility (BSRF). In this process, the Cross-Relaxation Energy Transfer (CRET) occurs via down conversion from the Gd^{3+} to Eu^{3+} ions. From the PL emission spectra monitored under the different excitation wavelength, the CRET process with visible Quantum Cutting (QC) was found to be 114% at the excitation wavelength of 246 nm.

Keywords: Visible Quantum Cutting, Down-Conversion, Quantum Efficiency (QE), Mercury Free Fluorescent Lamps (MFFL)

1. Introduction:

Visible Quantum Cutting (QC) is the phenomenon in which one high energy VUV or UV photon absorbed by the phosphors and its cuts in to two or more low energy visible photons via Down Conversion (DC) in which we got Quantum Efficiency greater than 100%. The fluoride host doped with rare earth are recognized as a more effective phosphors that find numerous applications including bioimaging [1-4]. From the literature review, it was found that the rare earth doped host $KMgF_3$ is effective luminescence material. $KMgF_3$-based luminescent phosphor are doped with rare earth or other activators showing the variability of luminescence phenomena. Such types of compounds are suitable for optical martials in UV or VUV regains. Therefore, these materials are used as VUV transparent materials for the subsequent generation of lithographic technology [5], as an emitter of light in VUV region [6,7], and electro-optical applications [8]. The photon cascade emission in Pr^{3+}-doped perovskite $KMgF_3$ was observed by Sokolska et al [9]. The properties of photoluminescence (PL) and Thermoluminescence (TL) have been widely deliberate in $KMgF_3$:Mn^{2+} [10-13] and also in $KMgF_3$: Lu, [14,15]. The PL spectra of Cu^{+}, Ni^{2+} doped $KMgF_3$ [16-18], $KMgF_3$:Cr^{3+} [19,20], $KMgF_3$:Sm^{2+} [21], and $KMgF_3$:Sm^{3+} [22] have been reported.

Impressed by the above work, Gd-Eu-doped and co-doped $KMgF_3$ phosphors were synthesized by a wet chemical method. In the present work, the pure crystal structure of synthesized phosphor was analyzed by XRD techniques. The PL properties of the synthesized phosphors are investigated under UV-VUV and visible regions. The quantum cutting and cross-relaxation energy transfer mechanism in the co-doped $KMgF_3$ system is also analyzed.

2. Experimental :

The phosphors $KMgF_3$: Gd^{3+}, Eu^{3+} is the first time prepared by a wet chemical method followed by RAP. The primary advantages of this method are comparatively low-temperature, higher controllability, low cost, and time-saving. The starting chemical magnesium nitrate ($MgNO_3$) (99.99% A.R.), and potassium nitrate KNO_3 (99.99% A.R.) are used as precursors, and Gadolinium Oxide (Gd_2O_3) (Loba 99.9%) and Europium Oxide (Eu_2O_3) (Loba 99.9%) are used as a dopant. The precursors and dopant were taken in a Teflon beaker and dissolved in the least amount of HNO_3. The solution was heated to 100 °C and dried completely to get an aqueous solution of KMg $(NO_3)_3$: Gd, Eu. By adding 20 ml of double distilled (DD) water to the solution and stirring, Hydrofluoric acid (HF) was added dropwise to get white precipitated. The precipitate was washed and filtered then heated on a hot plate (80°C) to get dried white powder.

The white dry powder was put in the glass tube with stopper and 1% wt. of RAP agent was added. In this process, we used ammonium fluoride as a RAP agent. Put the tube in furnace and heated slowly to 500 ◦C for 2 hr. The sample was removed from the tube and crush it, after that the powder was put in to a preheated graphite crucible heated to an 800 ◦C for 3 hr. Subsequent the materials was quickly slaked to room temperature. Jaiswal *et al* &. Belsare *et al*. well discuss the whole process in his literature [23-25].

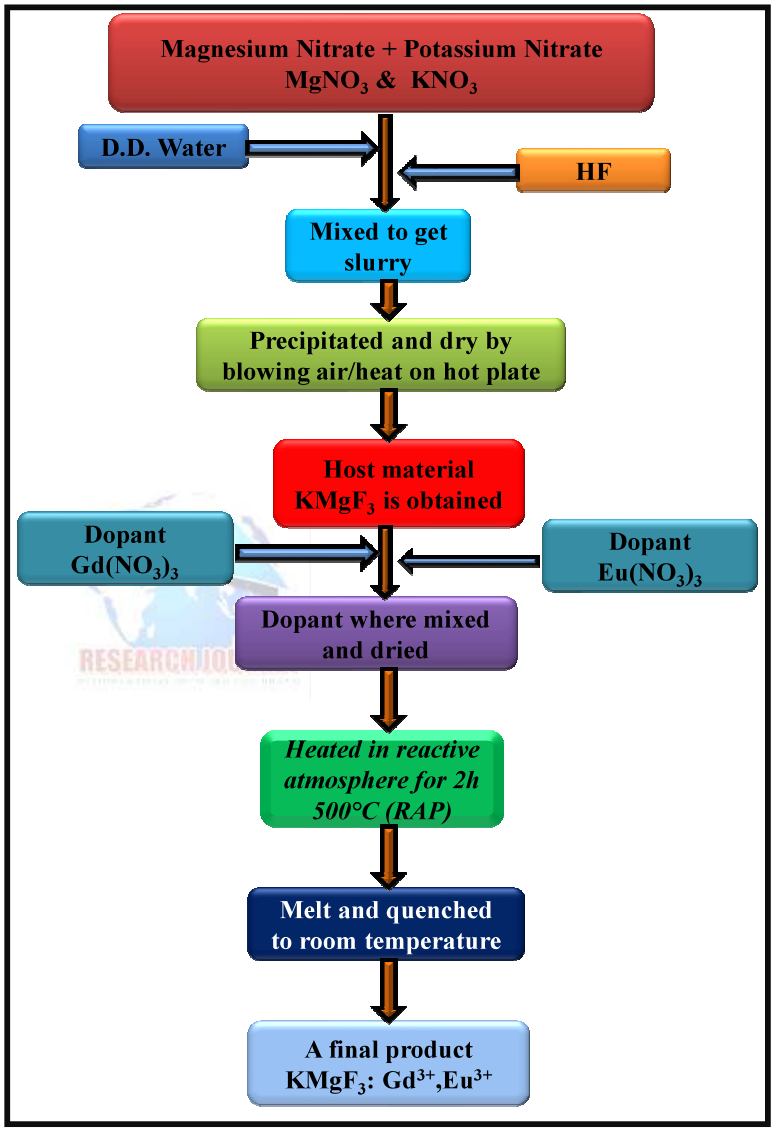

Fig. 1. Flow chart denoted the whole process elaborate in the flow chart

The chemical reaction of the synthesis process is shown below:

$$KNO_3 + (0.98\text{-}x)\ Mg(NO_3)_2 + 2HF + 0.5\ Gd_2O_3{}^* + 0.5\ Eu_2O_3{}^* \xrightarrow{\Delta} K\ Mg_{(0.98\text{-}X)}F_3{:}\ {}_{0.02}Gd^{3+}\ {}_{X}Eu^{3+} + \text{Gases product } (H_2O, NH_3 \text{ and } NO_2)$$

(x = 0.001, 0.005, 0.01, 0.02) {*In stock solution form 1gm≡100ml}

The whole procedure elaborate in the reaction was denoted in flow chart as shown in fig. 1

3. Result and Discussion:

3.1 Explanation of the Structure:

Fig. 2 shows the XRD pattern of the synthesized pure host material $KMgF_3$ and doped material $KMg_{0.97}F_3{:}_{0.02}Gd^{3+}$, $_{0.01}Eu^{3+}$ powder. All the major and minor peaks in XRD can be agreed well with the standard data from the ICDD file (01-086-2480) with space group: Pm3m [221]. Therefore, XRD confirms the samples (host as well as with dopant) obtained under the wet chemical method are in a pure cubic phase.

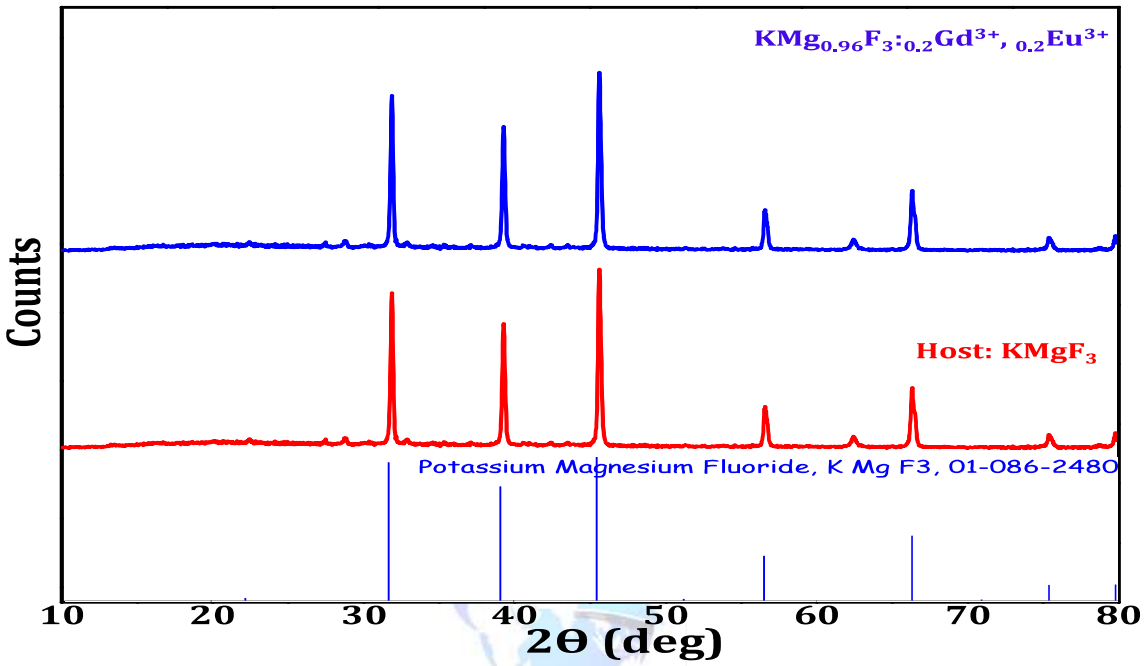

Fig. 2. The X-ray diffraction pattern of the prepared $KMgF_3$ doped and undoped material

3.2. Spectral properties of the synthesized phosphors

Firstly, we examined the concentration quenching in the $KMgF_3$ host doped Gd^{3+} as a sensitizer. From Fig.3 it can be stimulated that 0.02 moles of Gd^{3+} ions in the $KMgF_3$ crystal, show an optimal intensity peak at 311/312 nm under the 273 nm excitation wavelength.

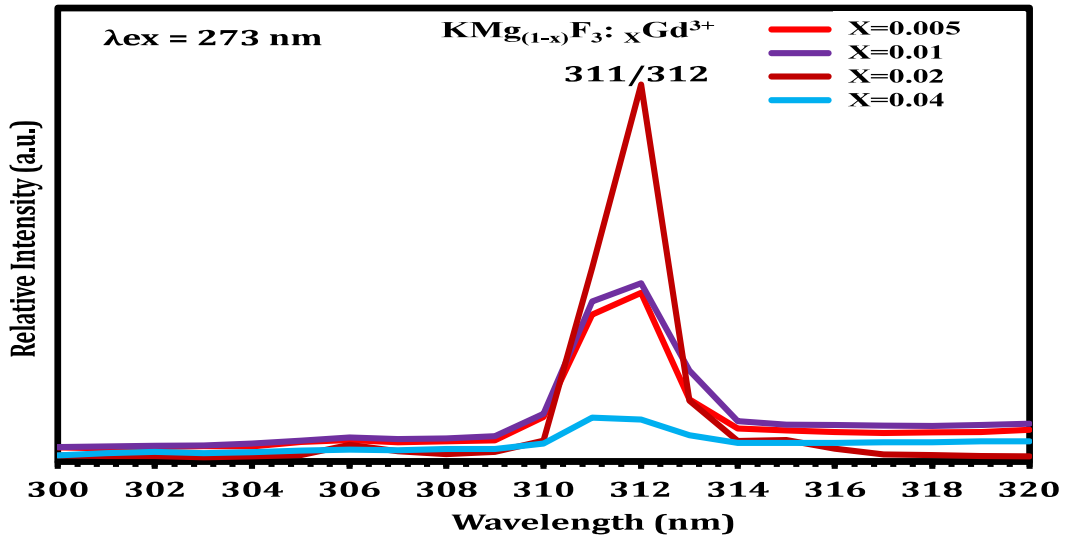

Fig. 3. Emission spectra of $KMgF_3$ host doped Gd^{3+} as a sensitizer monitored at 273 nm

The luminescence characteristics of $KMg_{(0.98-X)}F_3$: $_{0.02}Gd^{3+}$ $_XEu^{3+}$ phosphors with different Eu-doping contents are discovered in totally identical synthesizing conditions. The PL emission and excitation spectra under the VUV-UV range using synchrotron radiations for synthesized phosphors were studied:

3.2.1. Excitation spectra:

Fig. 4 shows the excitation spectrum of K $Mg_{(0.98-X)}$ F_3: $_{0.02}Gd^{3+}$ $_XEu^{3+}$ with different Eu concentration under the emission wavelength of 611 nm. The excitation peaks are attributed to excitation lines peaking nearly at about 207 nm responsible for the $^8S_{7/2}\rightarrow{}^6G_J$ transition. Similarly, the broadband from 217 to 266 nm is responsible for the $^8S_{7/2}\rightarrow{}^6D_J$ transition maximum peaking at 254, 251, 246, and 241 nm for x = 0.001, 0.005, 0.01 and 0.02 concentration of Eu^{3+} respectively as shown in Fig 4. The concentration quenching in K $Mg_{(0.98-X)}$ F_3: $_{0.02}Gd^{3+}$ $_XEu^{3+}$ was found at 0.02 moles of Eu concentration for the $^8S_{7/2}\rightarrow{}^6D_J$, ^6I_J transition only. The sharp excitation lines' peak maximum at about 273 may be ascribed to the shifting $^8S_{7/2}\rightarrow{}^6I_J$ of Gd^{3+}.

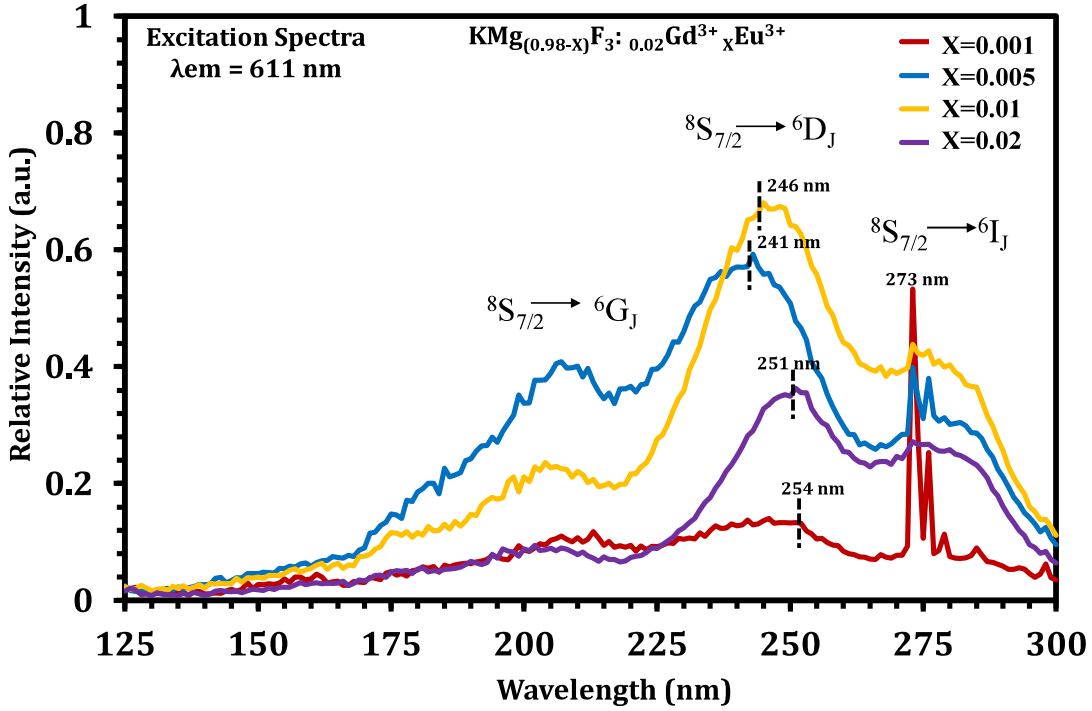

Fig. 4. Excitation spectrum of K $Mg_{(0.98-X)}$ F_3: $_{0.02}Gd^{3+}$ $_X$ Eu^{3+} monitored at 611 nm.

3.2.2. Emission Spectra

Fig. 5 (a) shows the emission spectra of K $Mg_{(0.98-X)}$ F_3: $_{0.02}Gd^{3+}$ $_X$ Eu^{3+} ($0.001 \leq X \leq 0.02$) in the range of 450-750 nm under the $^8S_{7/2}\rightarrow{}^6D_J$ of Gd^{3+} excitation maximum peaking at 254, 251, 246, and 241 nm for x = 0.01, 0.05, 0.1, and 0.2 moles concentration of Eu^{3+} respectively. The line peaks of emission spectra of Eu^{3+} at around 593, 618, 650, and 700 nm equivalent to $^5D_0\rightarrow{}^7F_J$ (J=1, 2, 3, 4) transition respectively, and the $^5D_1 \rightarrow {}^7FJ_{=0,1,2,3}$ transition crests of Eu^{3+} are far feebler than those of $^5D_0\rightarrow{}^7F_J$ transition are shown in figs 5. Fig. 5 (b) illustrations of emission spectra of K $Mg_{(0.98-X)}$ F_3: $_{0.02}Gd^{3+}$ $_X$ Eu^{3+} ($0.001 \leq X \leq 0.02$) under the $^8S_{7/2}\rightarrow{}^6I_J$ of Gd^{3+} excitation of wavelength 273 nm. If we compare the emission peak intensities in figs. 5 (a) and (b), we observed that in figs. 5, the emission strength of the $^5D_0$ to $^7F_1$ conversion is not as much the $^5D_0$ to $^7F_2$ transition. In fig. 5 (b), at an excitation of 273 nm, the

emission intensity of the $^5D_0$ to $^7F_1$ transition is greater than that of $^5D_0$ to $^7F_2$ transition. The concentration quenching in K Mg $_{(0.98-X)}$ F_3: $_{0.02}Gd^{3+}$ $_X$ Eu^{3+} at 0.02 of Eu concentration was also observed in emission spectra as shown in figs. 5 (a) and (b).

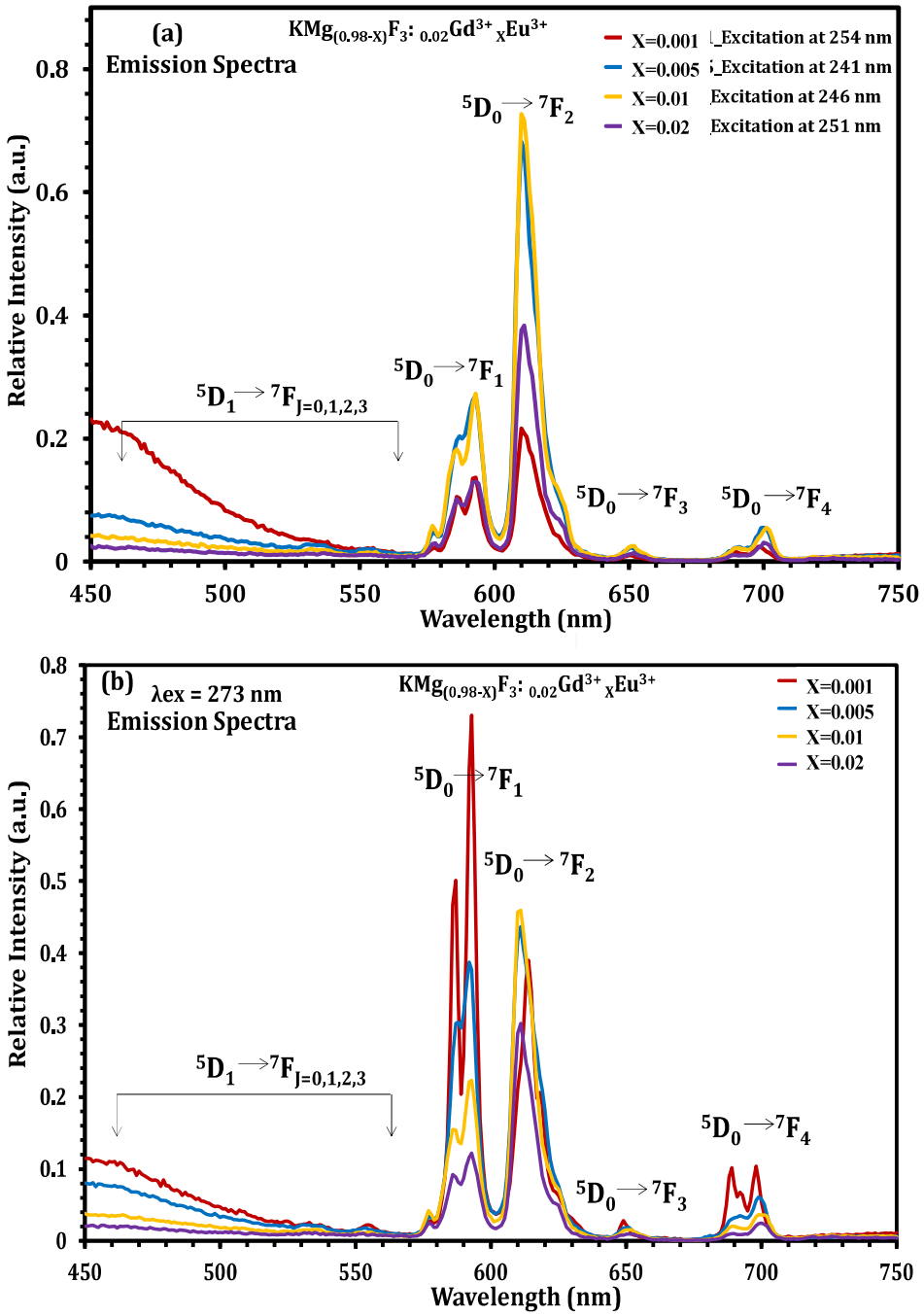

Figs. 5 (a) and (b): Emission spectra K Mg $_{(0.98-X)}$ F_3: $_{0.02}Gd^{3+}$ $_X$$Eu^{3+}$ at the different excitation wavelength

3.2.3 Energy transfer and quantum cutting

The maximum intensity was observed for the 0.01 moles of Eu concentration in the synthesized phosphor. Therefore, emission spectra of K $Mg_{0.97}$ F_3: $_{0.02}Gd^{3+}$ $_{0.01}Eu^{3+}$ are only considered for the study of ET process and QE.

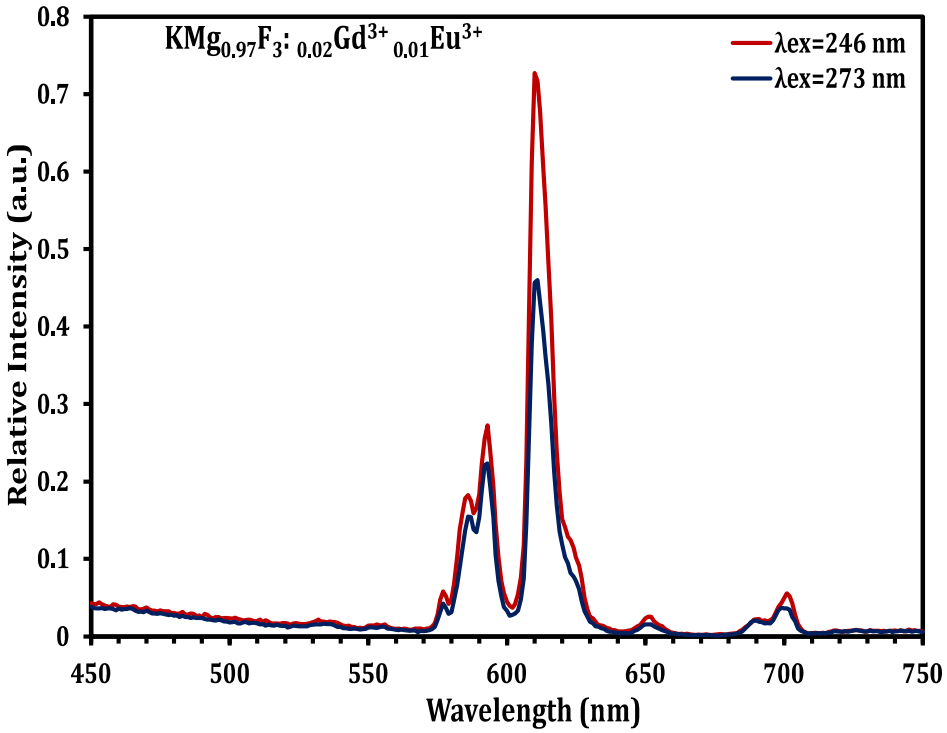

Fig 6: PL emission spectra of K $Mg_{0.97}$ F_3: $_{0.02}Gd^{3+}$ $_{0.01}Eu^{3+}$ monitored at 246 and 273 nm

Fig. 6 shows the PL emission spectra of K $Mg_{0.97}$ F_3: $_{0.02}Gd^{3+}$ $_{0.01}Eu^{3+}$ in the range of 450-750 nm supervised by 246 and 273 nm respectively. Thus, a assessment of the $^5D_0/^5D_{1,2,3}$ emission intensity ratio upon exciting in Gd^{3+} ^6G_J and ^6P_J (or ^6I_J, ^6D_J) levels may be used for the calculation QE via CRET. We have to find the occurrence of energy transfer and calculation of the extra QE via cross-relaxation energy transfer (CRET) used by the formula given by Wegh et al. [25-28]

$$\frac{P_{CR}}{P_{CR}+P_{DT}} = \frac{R(^5D_0 / {}^5D_{1,2,3})_{^6G_J} - R(^5D_0 / {}^5D_{1,2,3})_{^6I_J}}{R(^5D_0 / {}^5D_{1,2,3})_{^6I_J} + 1}$$

Where P_{CR} is the prospect for cross relaxation, P_{DT} is the prospect for the direct transfer from Gd^{3+} to Eu^{3+}. R ($^5D_0/^5D_{1,\,2,\,3}$) is the $^5D_0$ and $^5D_{1,\,2,\,3}$ emission integral intensities ratio. The subscript (^6G_J or ^6I_J) represents the excitation level for which the ratio is observed.

From the emission spectra, at the excitation wavelengths 246, and 273 nm, the value of R ($^5D_0/^5D_{1,\,2,\,3}$) ^6G_J and ($^5D_0/^5D_{1,\,2,\,3}$) ^6I_J can be calculated at 3.7959 and 3.1770, respectively. Therefore, the value of $P_{CR}/P_{CR} + P_{DT}$ is 0.14. It means that there are very minute i.e. **14** % Gd^{3+} ions in the ^6G_J excited state settle down through a two-step energy transfer emitting two visible photons in this method. So, a QE of 114 % can be obtained.

4. The SPD Spectra and CIE Color Coordinates

The color excellence of the phosphor will be generally restrained by the CIE chromaticity coordinate (x y). As per the emission spectrum of K $Mg_{0.97}$ F_3: $_{0.02}$ Gd^{3+} $_{0.01}Eu^{3+}$, the CIE coordinate is found to be (0.5505 and 0.3503). The Spectral Power Distribution (SPD) input spectra of K $Mg_{0.97}$ F_3: $_{0.02}$ Gd^{3+} $_{0.01}Eu^{3+}$, fitted to the CIE 1931 chromaticity diagram is shown in fig. 7

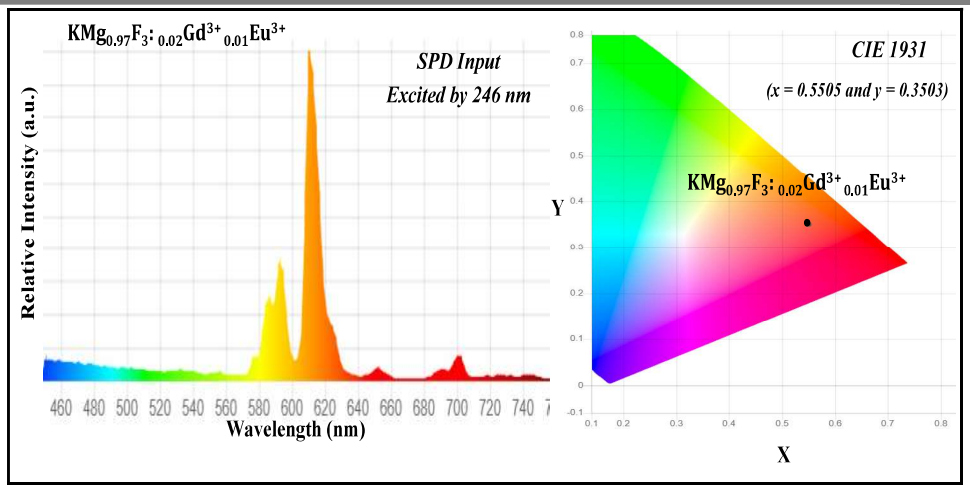

Fig. 7. SPD input and CIE chromaticity coordinates of red phosphor K $Mg_{0.97}$ F_3: $_{0.02}$ Gd^{3+} $_{0.01}Eu^{3+}$

4. Conclusions:

The $KMgF_3$ inorganic material doped and co-doped with Gd^{3+} and Eu^{3+} is magnificently synthesized through wet chemical method tailed by RAP. The phase purity is analyzed by the XRD technique and it is found to be a cubic phase. The CRET process via down conversion from the Gd^{3+} to Eu^{3+} ions are observed. The visible QE is calculated and it is found to be 114% under the excitation at 246 nm in $KMgF_3$: Gd^{3+}, Eu^{3+} phosphor. Hence the phosphor might be a probable application in MFFL.

Acknowledgments:

We are thankful to scientist of 4B8 VUV spectroscopy beamline, Beijing Synchrotron Radiation Facility (BSRF), Chaina for providing accesses to recording VUV radiation on beamline 4B8 using remote access mode. The author also that full to the head department of Physics Sant Gadge baba Amravati university, Amravati, for providing the XRD facility for this work.

References:

1. D. Chen, Z. Wan, Y. Zhou, P. Huang, and Z. Ji, J. Alloys Compd. **654**, 2016, pp. 151–156. https://doi.org/10.1016/j.jallcom.2015.09.146.
2. D. Chen and P. Huang, Dalton Trans. **43**/29, 2014, pp. 11299–11304 https://doi.org/10.1039/c4dt01237b.
3. D. Chen, Z. Wan, Y. Zhou, X. Zhou, Y. Yu, Jiasong Zhong, Mingye Ding, and Z. Ji, A.C.S. Appl. Mater. Interfaces **7**/34, 2015 pp. 19484–19493. https://doi.org/10.1021/acsami.5b06036.
4. D. Chen, L. Liu, P. Huang, Mingye Ding, Jiasong Zhong, and Z. Ji, J. Phys. Chem. Lett. **6**/14, 2015, pp. 2833–2840 https://doi.org/10.1021/acs.jpclett.5b01180.
5. T. Nishimatsu, N. Terakubo, H. Mizuseki, Y. Kawazoe, D. A. Pawlak, and K. Shimamura and T.Fukuda Jpn. J. Appl. Phys. Letts. 41, 2002, pp. 365.
6. K. Yamanoi, R. Nishi, K. Takeda, Y. Shinzato, M. Tsuboi, *et al*, Opt. Mater. **36**/4, 2014, pp. 769–772. https://doi.org/10.1016/j.optmat.2013.11.023.
7. M. Yanagihara, M. Z. Yusop, M. Tanemura, S. Ono, T. Nagami, *et al*, A.P.L. Mater. **2**/4, 2014, pp. 046110. https://doi.org/10.1063/1.4871915.

8. T. Fukuda, K. Shimamura, A. Yoshikawa, and E. G. Villora, Opto Electron. Rev. **9**, 2001, pp. 109.
9. Sokólska and S. Kück, Chem. Phys. **270**/2, 2001, pp. 355–362. https://doi.org/10.1016/S0301-0104(01)00408-6.
10. M. A. Young, E. E. Kohnke, and L. E. Halliburton, J. Phys. C: Solid State Phys. **9**/18, 1976, pp. 3515–3522. https://doi.org/10.1088/0022-3719/9/18/018.
11. S. Kück and I. Sokólska, J. Phys.: Condens. Matter **18**/23, 2006, pp. 5447–5457. https://doi.org/10.1088/0953-8984/18/23/016.
12. F. Rodríguez, H. Riesen, and H. U. Güdel, J. Lumin. **50**/2, 1991, pp. 101–110. https://doi.org/10.1016/0022-2313(91)90024-P.
13. R. Alcala, N. Koumvakalis, and W. A. Sibley, Phys. Stat. Sol. (a) **30**/2, 1975, pp. 449–456. https://doi.org/10.1002/pssa.2210300203.
14. J. Marcazzó, E. Cruz-Zaragoza, P. R. González, M. Santiago, and E. Caselli, Radiat. Meas. **71**, 2014, pp. 262–264. https://doi.org/10.1016/j.radmeas.2014.03.002.
15. P. R. Gonzalez, C. Furetta, J. Marcazzo, E. Cruz-Zaragoza, and L. Perez, Cruz Appl. Radiat. Isotopes 79, 2013, pp. 67
16. S. Lizzo, A. Meijerink, G. J. Dirksen, and G. Blasse, Chem. Phys. Lett. **253**/1–2, 1996, pp. 108–112. https://doi.org/10.1016/0009-2614(96)00216-3.
17. J. Ferguson, H. J. Guggenheim, and D. L. Wood, J. Chem. Phys. **40**/3, 1964, pp. 822–830. https://doi.org/10.1063/1.1725212.
18. W. E. Vehse, K. H. Lee, S. I. Yun, and W. A. Sibley, J. Lumin. **10**/3, 1975, pp. 149–162. https://doi.org/10.1016/0022-2313(75)90044-7.
19. J. M. García-Lastra, P. García-Fernández, M. T. Barriuso, J. A. Aramburu, and M. Moreno, J. Phys. Chem. A **118**/12, 2014, pp. 2377–2384. https://doi.org/10.1021/jp5010067.
20. M. Q. Kuang, S. Y. Wu, X. F. Hu, G. L. Li, and H. Y. Zu, Acta Phys. Pol. A **125**/5, 2014, pp. 1224–1228. https://doi.org/10.12693/APhysPolA.125.1224.
21. W. S. Zhang, H. L. Pan, G. G. Zhou, C. J. Shao, C. D. Lin, and G. W. Lu, J. Synth. Cryst. **42**, 2013, pp. 2536.
22. S. Ping, M. Yang, Z. Wen-Chen, and L. Hong-Gang, Phys. B **420**, 2013, pp. 1.
23. P. D. Belsare, C. P. Joshi, S. V. Moharil, V. K. Kondawar, P. L. Muthal, and S. M. Dhopte, J. Alloys Compd. **450**/1–2, 2008, pp. 468–472. https://doi.org/10.1016/j.jallcom.2006.11.008.
24. S. Jaiswal, N. Sawala, P. Nagpure, V. Bhatkar, and S. Omanwar, Mater Sci: Mater Electron 28, 2017, pp. 2407–2414.
25. S. Jaiswal, P. Nagpure, and S. Omanwar, Journal of Biological and Chemical Luminescence, 2021, pp. 1–7.
26. S. K. Omanwar, S. R. Jaiswal, N. S. Sawala, K. A. Koparkar, and V. B. Bhatkar, Mater. Discov. **7**, 2017, pp. 15–20. https://doi.org/10.1016/j.md.2017.05.003.
27. S. K. Omanwar, S. R. Jaiswal, N. S. Sawala, K. A. Koparkar, P. A. Nagpure, and V. B. Bhatkar, St. Petersburg Polytech. Univ. J. Phys. Math. **3**, 2017, pp. 218–224.
28. S. R. Jaiswal, N. S. Sawala. P.A., and S. K. Nagpure Omanwar, Adv. Mater. Res. **1171**, 2022, pp. 17–24.